Environmental Science and Pollution Research (2021) 28:12475–12489
https://doi.org/10.1007/s11356-020-11256-3

RESEARCH ARTICLE

Sorption of U(VI), Mn (II), Cu(II), Zn(II), and Cd(II) from multi-component phosphoric acid solutions using MARATHON C resin

Mohamed H. Taha [1]

Received: 15 May 2020 / Accepted: 13 October 2020 / Published online: 20 October 2020

Abstract

Crude phosphoric acid is a vital component used in making phosphate fertilizers. Depending on the processes used in producing the crude phosphoric acid, it usually contains organic and inorganic contaminants. To make environmentally friendly phosphate fertilizers, these contaminants must be removed from the crude phosphoric acid stock used in making fertilizers. In this paper, commercially available strong cation exchange resin, Marathon C, was used to study the adsorptive removal of U(IV), Mn(II), Cd(II), Zn(II), and Cu(II) from synthetic multi-component phosphoric acid solutions and commercial crude phosphoric acid. Important parameters on the adsorption process such as the effects of contact time, initial metal ion concentration, sorbent dose, and concentration of phosphoric acid were investigated. The results suggested that the adsorption process reached equilibrium within 240 min for the five metal ions studied and the resin had adsorptive affinity for the metal ions in the order of U(IV) > Zn(II) > Cu(II) > Mn(II) > Cd(II). The results from the kinetics and isotherm models from the studies are very consistent with pseudo-second-order kinetic and Langmuir isotherm models. Simultaneous adsorptive removal of metal ions from the crude phosphoric acid strongly suggests that the Marathon C resin could be used in removing toxic metal ions from crude phosphoric acids used in making phosphate fertilizer.

Keywords Sorption · Uranium · Multi-component solution · Phosphoric acid · Marathon C resins

Introduction

Phosphorus, together with potassium and nitrogen, are important nutrients for corps development and growth. Modern farming is depending mainly on phosphate fertilizers, which are produced from phosphate rock, for food production to meet the world population growth. Thus, phosphorus is considered as an essential building block of the food security system (Geissler et al. 2015; Steiner et al. 2015; Geissler et al. 2019).

The world demand for phosphate rock is increasing because of the increase of the world population as well as food demand (Ridder 2012). The United Nations reported that food production worldwide has been increased by 70% in past decades due to the observed inflation in the world population to become over 9 billion by 2020. Consequently, the global demand for phosphate rock will increase as a result of the world population growth (van Kernebeek et al. 2018; Schoumans et al. 2015).

Phosphate rocks are mainly classified as (i) sedimentary phosphate deposits (which represent about 75% of the world phosphate rock that exist in Egypt, Jordan, and the USA) and (ii) igneous phosphate deposits (about 20% exists in Brazil, South Africa, and Russia) (Petr Ptáček 2016; Fayiga and Nwoke 2016). Phosphate rocks contain remarkable concentrations of heavy metals as well as radioactive elements such as uranium (U), lead (Pb), arsenic (As), manganese (Mn), copper (Co), zinc (Zn), and cadmium (Cd). These elements are non-biodegradability, bio-accumulation, and classified as carcinogenic (Mar and Okazaki 2012; Gaafar et al. 2016). The concentration of these toxic elements in phosphate rock deposits is different from one type to another (Fayiga and Nwoke 2016; Mar and Okazaki 2012).

To a large extent, phosphoric acid is manufactured through the wet process using concentrated sulfuric acid. In such

Responsible Editor: Tito Roberto Cadaval Jr

✉ Mohamed H. Taha
dr.mohamedp@gmail.com

[1] Nuclear Materials Authority, P.O. Box 530, El Maddi, Cairo, Egypt

process, sulfuric acid is reacting with the phosphate rock and produces phosphoric acid (liquid phase) and phosphogypsum (solid phase). Most of the radioactive and hazardous elements move to the liquid phase, during the production stage, and consequently to the phosphate fertilizers (Hocking 2005). Despite the importance of phosphate fertilizers, the long-term applications of phosphate fertilizers result in the accumulation of toxic heavy metals and radionuclides in the soil and subsequently to both the food chain as well as the aquatic ecosystem (Fayiga and Nwoke 2016; Mar and Okazaki 2012).

Several techniques have been tested for the separation of toxic as well as radioactive elements from industrial phosphoric acid, for instance, crystallization (Chen et al. 2012), *electrodialysis* (ED) (Machorro et al. 2013), membrane extraction (Elleuch et al. 2006), precipitation (Mousa et al. 2013; Al-Harahsheh et al. 2017), solvent extraction (Mohamed H. Taha 2017; Bahrpaima 2017), and solid-liquid extraction (Hinojosa Reyes et al. 2001; El-Sofany et al. 2009). The selection of the appropriate technique is depending on mainly the concentration of the undesirable elements and phosphoric acid (Elleuch et al. 2006). The application of these approaches was limited due to numerous disadvantages, for example, environmental pollution by some by-products, difficulty in recovering all the solvent from both the raffinate and the purified acid, high costs of organic solvents, and limited efficacy (Elleuch et al. 2006; El-Bayaa et al. 2011). However, solid–liquid technology exhibits higher selectivity, cost-efficient technology, and eco-friendly process for heavy metal removal (El-Bayaa et al. 2011; Jaafari and Yaghmaeian 2019a, b; Jaafari and Yaghmaeian 2019a, b; Dariush Naghipour et al. 2018).

Different solid materials were studied for phosphoric acid clarification, such as solvent impregnated charcoal (El-Sofany et al. 2009), activated bentonite (Taha et al. 2018), and white silica sand (El-Bayaa et al. 2011). However, the above materials are to somewhat cumbersome in reuse and recovery (Nagaphani Kumar et al. 2010; Hérès et al. 2018). Commercially, ion exchange resins are characterized by their heat and acid resistance nature as well as providing the option of being reused for several sorption-desorption cycles (Nagaphani Kumar et al. 2010; Hérès et al. 2018). Ion exchange resins have been investigated for the recovery of U(VI) and REEs (rare earth elements) from phosphoric acid (Nagaphani Kumar et al. 2010; Hérès et al. 2018). So far, limited trails were performed in laboratory for the separation of heavy and toxic metals from phosphoric acid solutions using resins. Nevertheless, these trail attempts have never been applied industrially (KOOPMAN et al. 1999; Cheira 2015).

In this regards, the main goal of this work is investigating the sorption of U(VI), Mn (II), Cd(II), Zn(II), and Cu(II) ions from multi-component phosphoric acid solutions using commercially available strong cation exchange resin (MARATHON C–sulfonic group resin) in order to propose a proper and cost-effective process for the production of eco-friendly phosphate fertilizers. The impact of numerous variables that may affect the sorption process, such as contact time, phosphoric acid concentrations, sorbent dose, and reaction temperature, is going to be investigated through this study. Furthermore, isotherms, kinetics, and thermodynamics of the introduced sorption process via using the aforementioned resin will be of a particular focus during the current investigation.

Experimental

Materials

Dowex Marathon C resin, a gel type strong acid cation exchange resin with polystyrene divinylbenzene matrix, was purchased from Sigma-Aldrich (Germany). The resin was firstly pre-conditioned in sodium hydroxide, then in hydrochloric acid solution, and finally in deionized water before being used in this investigation (Hagag et al. 2017). The main characteristics as well as the function groups of Marathon C resin are given in Table 1 and Fig. 1. All the utilized chemicals and reagents were AR grade. $UO_2(NO_3)_2$, $MnSO_4$, $CuSO_4$, $CdSO_4$, and $ZnSO_4$ were obtained from Fluka Chemika (Switzerland) and were used for preparing the synthetic metal ion stock solution 1000 ± 1 mg/L. Analytical grade phosphoric acid (88%, specific gravity 1.75) was purchased from Merck KGaA (Darmstadt, Germany) and utilized for the study of synthetic solutions. Multi-component solution samples of different phosphoric acid concentrations were synthesized freshly by adding certain volumes of the metal ion stock solutions with different volumes of pure concentrated phosphoric acid and double-distilled water. Crude phosphoric acid, purchased from Abu Zaabal Company for Fertilizer and

Table 1 The physical and chemical characteristics of Dowex Marathon C resin

Appearance	Uniform particle size spherical beads
Functional group	Sulfonic acid
Matrix	Styrene-DVB, gel
Total exchange capacity (eq/L)	1.8
Ionic form	H+ form
Moisture retention	50–56%
Particle size range	600 ± 50 μm
Specific gravity	1.2
Temperature limit	120 °C
pH range	0–14
Regenerate	4–8% HCl, 1–8% H_2SO_4, 8–12% NaCl

Chemical Materials (AZFC), is used for experimental application without any purification processes. The chemical analyses of crude phosphoric acid were performed at the Nuclear Materials Authority and are given in Table 2.

Instrumentation

Atomic Absorption Spectrometer GBC 932 AA (UK) with a double-beam system, equipped with hollow cathode lamps, was used for the determination of Mn, Cu, Zn, and Cd ion concentration. A double-beam spectrophotometer of high-resolution power (Shimadzu UV-Visible recording spectrophotometer type UV-60A) was used for the determination of uranium concentration. A NUVE thermostatic shaker was used for equilibrium experiments.

Batch adsorption experiments

The sorption experiments have been achieved via a batch-wise route using 10-mL polyethylene tubes. The sorption experiments were performed in duplicate and ~5% relative errors were accepted. Despite that the pH effect on the metal binding is the primary step in the design of a sorbent process, in the present study, the strategy focused on the development of preferred process based on unchanged pH (the only variation dealt with the effect of phosphoric acid dilution in the relevant section investigating the effect of acid concentration). The impact of important variables on the sorption process such as contact time (2–600 min), sorbent dose (0.5–5 g/L), phosphoric acid molarity (1–6 M), and initial metal ion concentration (20–300 mg/L) have been investigated. A fixed weight of Marathon C resin was shaken with a fixed volume of a synthetic phosphoric acid solution that contains 50 mg/L of each metal ions in a thermostatic shaker bath at 298 ± 1 K. In most cases, phosphoric acid concentration was 2.0 M. To confirm that complete equilibrium achieved, the experiments have been performed for 10 h. The solid sorbent was filtered out from the aqueous solution using filter membrane (pore size: 1.2 μm). After filtration, the residual concentrations of the Mn, Cu, Cd, and Zn ions have been measured using AAS while the concentration of uranium has been detected by using Arsenazo-III spectrophotometer method at 650 nm (Marczenko and Balcerzak 2000).

Table 2 Chemical specifications of crude phosphoric acid working sample

Constituents	Phosphoric acid
Concentration Wt.%	
P_2O_5	≈ 23.5
Fe_2O_3	1.2
CaO	0.34
SO_4	1.35
SiO_2	0.08
F	0.5
Concentration (ppm)	
Cd	10.5
Mn	580
Cu	53
Zn	183
U	41

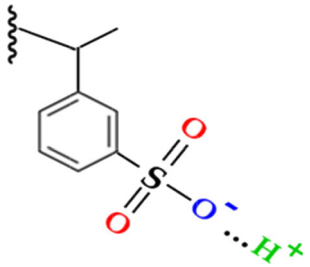

Fig. 1 Schematic of functional groups of the Marathon C resin

The difference between metal ion initial concentrations (Co, mg/L) and the concentration at equilibrium (Ce, mg/L) has been used to calculate the quantity of adsorbed ions on the resin (qe) according to the following relation:

$$q_t = C_o - C_e \times \frac{V}{m} \quad (1)$$

where q_t (mg/g) is the amount of ion sorbent at time t, V (L) is the of phosphoric acid solution volume, and m (g) is the resin mass. The distribution coefficient (K_d) could be described as the following:

$$K_d = \frac{C_o - C_e}{C_o} \times \frac{V}{m} \quad (2)$$

The metal ion sorption percent could be obtained

$$E\% = 100\% \times (1 - C_e/C_o) \quad (3)$$

Modeling of sorption process

Adsorption isotherm models

The adsorption isotherm (the adsorbate-adsorbent equilibrium properties) is important parameter for the improvement of the adsorption system and plant design. In this regards, the equilibrium data has been described using Freundlich, Langmuir, and Temkin models.

Freundlich isotherm equation Freundlich isotherm equation has been used to describe the sorption on heterogeneous surfaces (Hussein and Taha 2013). This model assumes that the sorption sites are exponentially distributed with respect to the sorption heat. The non-linear form of Freundlich isotherm

model can be expressed as (Al-Ghouti and Da'ana 2020)

$$q_e = K_F C_e^{1/n_F} \quad (4)$$

where K_F (mg/g) is corresponding to the Freundlich constant, and $1/n_F$ refers to the heterogeneity of the adsorbate sites.

Langmuir isotherm model Langmuir isotherm model is one of the most popular equations that have been used to describe the sorption phenomena (Foo and Hameed 2010). This model suggested that the sorption performed by monolayer sorption on a homogeneous surface without binding between adsorbed molecules. Langmuir model non-linear form is commonly expressed as the following (Al-Ghouti and Da'ana 2020):

$$q_e = \frac{q_m k_L C_e}{1 + k_L C_e} \quad (5)$$

where q_m (mg/g) is the maximum sorption capacity of Marathon C resin and k_L (L/mg) is the Langmuir constant which refers to the energy of adsorption and reflects the affinity of resin towards the metal ions.

Temkin isotherm equation Temkin isotherm equation considers the impact of resin–metal ion interactions on the adsorption process. Temkin model proposed that $\Delta\,^{\circ}_{ads}$ (the heat of adsorption) of all molecules in the layer is a function of the surface coverage (Ayawei et al. 2017). The non-linear form of Temkin equation is written as the following (Al-Ghouti and Da'ana 2020):

$$q_e = \frac{RT}{b_T} \ln K_T C_e \quad (6)$$

where R is the ideal gas constant (8.314 J/mol/K), T is the temperature (K), b_T is the Temkin constant that refers to the adsorption heat, and K_T (L/min) is the equilibrium binding constant.

Adsorption kinetic models

The uptake kinetics have been investigated to better understand the rate of adsorption and possible adsorption mechanism of U(VI), Mn(II), Cd(II), Zn(II), and Cu(II) ions using Marathon C resin. In this context, Lagergren, pseudo-second-order, Elvoich kinetic equations, as well as the intraparticle diffusion (Weber and Morris) equation has been applied to the adsorption data.

Pseudo-first order equation Pseudo-first-order equation (PFO) has been proposed by Largergren in 1898 to describe the sorption rate of solid-liquid phase adsorption systems in regards to the adsorption capacity (Largitte and Pasquier 2016). The non-linear form of PFO model used is (Marques et al. 2019)

$$q_t = q_1\left(1 - e^{-k1t}\right) \quad (7)$$

where q_1 (mg/g) is the estimated adsorption capacity by PFO model and $k1$ (min^{-1}) is Lagergren equation rate constant.

Pseudo-second-order model Pseudo-second order model (PSO) is also known as the McKay equation. This model is based on the sorption capacity of the solid phase. Additionally, it is assuming that chemisorption is the rate-determining step (Tan and Hameed 2017). The non-linear form of PSO model used is (Marques et al. 2019)

$$q_t = \frac{1}{\left(1|k_2 q_2^2\right) + (t|q_2)} \quad (8)$$

The initial adsorption rate, h (mol/g/h), and the half-equilibrium time, $t_{1/2}$ (h) for Marathon C resin were obtained from Eqs. 9 and 10 (Tan and Hameed 2017).

$$h = k_2 q_e^2 \quad (9)$$

$$t_{\frac{1}{2}} = \frac{1}{k_2 q_e} \quad (10)$$

where k_2 (min^{-1}) is the McKay equation rate constant and q_2 (mg/g) is the estimated adsorption capacity by PSO model.

Elovich equation Elovich equation has been proposed by Roginsky and Zeldovich in 1934 to describe the chemisorption adsorption reactions. The model proposes that the rate of solute adsorption exponentially decreases by the increase in the quantity of adsorbed solute (Wekoye et al. 2020; (Marques et al. 2019). Elovich equation could be expressed as the following:

$$q_t = \frac{1}{a} \ln(1 + abt)\Big) \quad (11)$$

where a (g/mg) is the desorption constant of Elovich model and b (mg/g/min) is referred to the initial velocity when $q_t = 0$.

Intra-particle diffusion model Intra-particle diffusion model (IPD) is also known as the Weber and Morris model. This model has been proposed in 1963 to describe the rate-limiting step during adsorption. Based on this model, the solute adsorption involves three processes: (1) film diffusion, (2) surface diffusion, and (3) pore diffusion. The surface and pore diffusion could occur simultaneously, so that film diffusion is an independent (Wu et al. 2009). The IPD equation is expressed as the following (Wu et al. 2009):

$$q_t = K_{id} t^{0.5} + C_i \quad (12)$$

where K_{id} (mg/g/min$^{0.5}$) is the rate constant and C is the thickness of the boundary layer.

Fitting the kinetic and isotherm models

The fitting of the kinetic and isotherm models has been tested by the non-linear regression Chi-square (x^2) (Eq. 12) and the average relative error (ARE) (Eq. 13) (Al-Ghouti and Da'ana 2020; Marques et al. 2019).

$$x^2 = \sum \left[\frac{\left(q_{exp} - q_{pred}\right)^2}{q_{pred}} \right] \quad (13)$$

$$ARE = \frac{100}{n} \sum_{1}^{n} \frac{\left|q_{exp} - q_{pred}\right|}{q_{exp}} \quad (14)$$

where q_{exp} and q_{pred} are the experimental and model predicted equilibrium capacity (mg/g), respectively, x^2 is the Chi-square coefficient, and n is the number of test points.

Results and discussions

In this section, the influence of main parameters on the sorption of U(VI), Mn(II), Cd(II), Zn(II), and Cu(II) from the synthetic phosphoric acid solution using commercial cation exchange resin Marathon C has been investigated. The sorption isotherms and kinetics have been investigated in order to figure out the sorption performance and disclose the underlying mechanisms. Finally, the application of the obtained results on an industrial crude phosphoric acid in order to obtain an eco-friendly phosphoric acid that can be subsequently used to obtain efficient phosphate fertilizers will undergo.

Effect of sorbent amount

Figure 2 describes the impact of Marathon C resin amount of addition on the sorption percent of multi cations, namely, U(VI), Mn(II), Cd(II), Zn(II), and Cu(II) from phosphoric acid solution. The experiments were performed at the following parameters: phosphoric acid molarity of 2.0 M, room temperature, metal ion initial concentration of 50 mg L^{-1}, and reaction time of 10 h, while the sorbent amount varied from 0.5 to 5.0 g/L. The exposed data show that the increase in sorbent amount extremely increases the sorption efficiency. The same effect has been observed for the five investigated metal ions. Numerically, the removal percent varied from 12.4 to 89.2% for Mn(II) with the variation of sorbent dose from 0.5 to 5.0 g/L. Within the same sorbent variation, the sorption percent has changed from 17.3 to 92.5% for Cu(II), from 27.8 to 96.4% for Zn(II), from 14.9 to 84.4% for Cd(II), and from 21.4 to 97.8% for U(VI). This behavior could be attributed to the

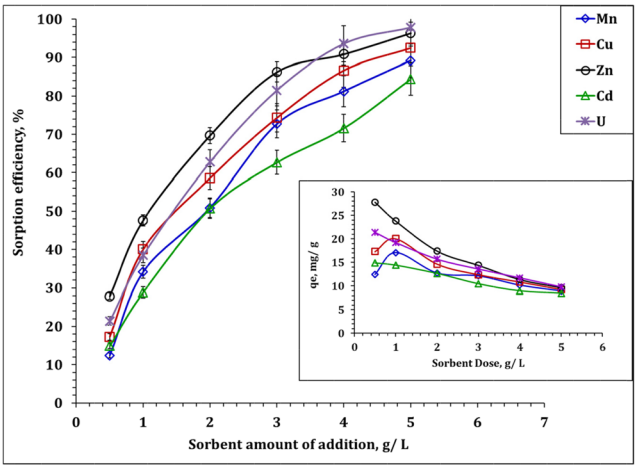

Fig. 2 Impact of sorbent dose on U(VI), Mn(II), Cd(II), Zn(II), and Cu(II) sorption efficiency and sorption capacity, % (4.0 g sorbent/L of 2.0 M phosphoric acid; temperature 298 K; 100 rpm)

increase in the available active binding sites by the increase of the sorbent dose, which in turn increases the rate of adsorption (Younes et al. 2018; Wang et al. 2017).

Despite the sorption efficiency increased with the increase in the sorbent dose, however, it is noticeable that the sorption capacity q_e for all metal ions is decreased (Fig. 2). This behavior could be due to clothing of the material, a lower increase in vacancy places could take place, thus a lowering in q_e value. Moreover, the low concentration of U(VI), Mn(II), Cd(II), Zn(II), and Cu(II) ions is not equivalent to the resin adsorption capacity and thereby decreased the q_e (Younes et al. 2018; Wang et al. 2017). The sorbent dose of 4.0 g/L has been chosen for further experiments to perform the sorption characterization.

Effect of initial concentration of metal ion

The sorption isotherms are essential to get the sorption capacity and generate the required data for the process up-scaling. In this regards, Dowex Marathon C resin was experimented for the elimination of U(VI), Mn(II), Cd(II), Zn(II), and Cu(II) from synthetic phosphoric acid solution containing different ion's initial concentrations. In practical, phosphoric acid solutions contain ion initial concentrations varied from 20 to 300 mg/L for each metal ion that has been contacted with the resin in solid/liquid ration equal 4.0 g/L, at room temperature for 10 h. The exposed results have been exhibited in Fig. 3 as a relation between sorption percent and the ion's initial concentration. Figure 3 declares that the sorption efficiency of the metal ions strongly depreciated with the increase in the initial metal ion concentration. In details, as the ion's initial concentration raised from 20 to 300 mg/L, the adsorption percent decreased from about 91 to 12.6% for Mn(II), from 96.8 to 14.8% for Cu(II), from 96.5 to 17.4% for Zn(II), from 86.2 to 9.7% for Cd(II), and from 99.1 to

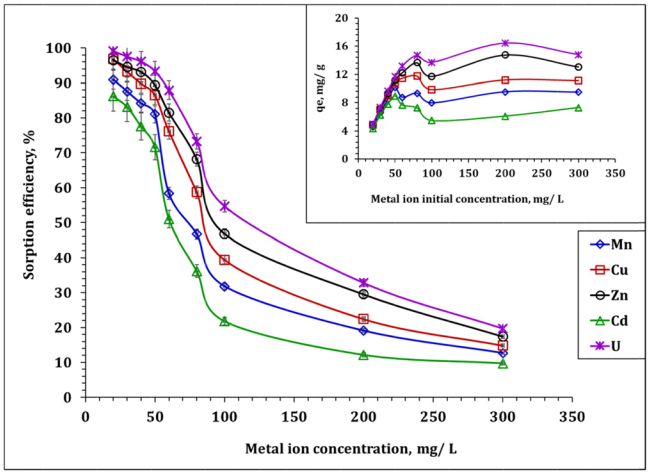

Fig. 3 Impact of initial concentration on U(VI), Mn(II), Cd(II), Zn(II), and Cu(II) sorption efficiency and sorption capacity, % (4.0 g sorbent/L of 2.0 M phosphoric acid; temperature 298 K)

19.7% for U(VI). In spite of the metal ion's sorption efficiency decreased with the metal ion's initial concentration increase, however, the resin sorption capacity was positively affected with the rise of the ion's initial concentration as shown in Fig. 3. The displayed data in Fig. 3 clear that the resin experimental maximum capacity is about 9.5, 11.1, 13.1, 7.3, and 16.4 for manganese, copper, zinc, cadmium, and uranium metal ions, respectively. Moreover, it is obviously clear that the resin has a higher tendency towards U(VI), then Cu(II), followed by Zn(II) and Mn(II), and the lowest affinity is for Cd(II).

The isotherm of U(VI), Mn(II), Cd(II), Zn(II), and Cu(II) ion adsorption from phosphoric acid solution using Marathon C resin has been investigated using the non-linear equations of Langmuir, Freundlich, and Temkin models. The equilibrium isotherm analysis is explored in Fig. 4. The isotherm parameters as well as X^2 and ARE values have been evaluated and presented in Table 3.

Table 3 Isotherm parameters of Langmuir, Freundlich, and Temkin models

	Mn	Cu	Zn	Cd	U
Langmuir model					
q_m (mg/g)	9.6	11.3	13.6	7.4	14.8
k_L (L/mg)	0.59	1.18	0.78	1.09	1.18
X^2	0.8	0.5	0.4	1.8	2.4
ARE (%)	6.8	5.8	4.6	14.1	8.2
Freundlich model					
$1/n_F$	11.0	9.5	6.3	28.5	8.1
k_F (mg/g) (mg/L)	5.99	6.57	6.73	6.00	9.09
X^2	2.1	3.0	3.0	2.3	2.1
ARE (%)	13.2	13.7	15.5	16.9	14.3
Temkin model					
b_T (J/mol)	1745.4	2545.8	1795.3	3474.0	1625.8
A_T (L/g)	16.9	645.1	308.3	499.3	351.0
X^2	3.0	2.5	2.1	3.2	1.2
ARE (%)	15.4	12.2	14.9	20.0	10.3

The mathematical treatment of the displayed results regards to the isotherm equations; Langmuir, Freundlich, and Temkin isotherm models have been presented in Table 3**.** The displayed data show that the Langmuir isotherm model supplies the lowest X^2 and ARE values. This reveals that the U(VI), Mn(II), Cd(II), Zn(II), and Cu(II) ion sorption from phosphoric acid solution using Marathon C resin is obeyed to Langmuir isotherm model. This indicates that the metal ion adsorption is homogeneous and each molecule possesses constant sorption activation energy and enthalpies (Younes et al. 2018). The maximum sorption capacity q_m of Mn(II), Cu(II), Zn(II), Cd(II)m and U(VI) ions are 9.6, 11.3, 13.6, 7.4, 14.8 mg/g, respectively. This confirms that Marathon C resin has a different affinity towards the investigated metal ions.

The sorbent affinity towards ions is highly affected by several parameters such as hydration ion radii, ion hydrolysis constant, metal ion electronegativity, and hydration energy (Lazarević et al. 2007; Vico 2003). Moreno et al. (2010) displayed the effect of the hydrated ionic radius on the affinity

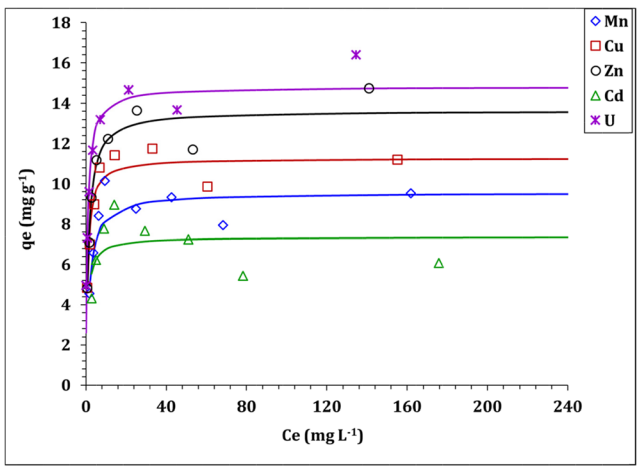

Fig. 4 Langmuir model plot for U(VI), Mn(II), Cd(II), Zn(II), and Cu(II) adsorption from phosphoric acid solution

of Cow bone charcoal (CBC) towards manganese, iron, nickel, and copper ions. Mihajlović et al. (2014) discussed the affinity of natural and modified zeolite towards $Pb^{2+} > Cd^{2+} > Zn^{2+}$ with respect to the hydrated cation radii, the hydration energy, and the ion electronegativity. Igwe and Abia (2007) reported the impact of ionic radii and the hydration energy (ΔH_{hyd}) on the selectivity of EDTA-modified maize cob towards Zn^{2+}, Cd^{2+}, Pb^{2+}. Khalili et al. (2013) attributed the affinity of Jordan bentonite towards Th(IV) > U(VI) to the ionic radii and metal ion hydrolysis constant (pK_h). Page et al. (2017) declared that the strength of the REE over Al and Fe(III) adsorption onto a sulfonic acid resin is affected by the cation hydration energy.

The ion radius of the hydrated metal ions could be arranged descendingly as the following: $UO_2(H_2O)_5^{2+}$ (1.08 Å) > $Cd(H_2O)_6^{2+}$ (0.96 Å) > $Mn(H_2O)_6^{2+}$ (0.86 Å) > $Cu(H_2O)_6^{2+}$ (0.80 Å) > $Zn(H_2O)_6^{2+}$ (0.74 Å) (Persson 2010). This means that the sorption affinity cannot be correlated to this parameter. This probably indicates that the ion radius of the hydrated metal ions has not a strong effect on the binding of the resin with the investigated ions. The studied ions could be ranked based on the hydration energy as the following sequence: U(VI) (− 3958 kJ/Mol) > Cu(II) (− 2100 kJ/Mol) > Zn(II) (− 2046 kJ/Mol) > Mn(II) (− 1841 kJ/Mol) > Cd(II) (− 1807 kJ/Mol) (Smith 1977; Khalili et al. 2013). Therefore, the sorption strength should be ranked as U(VI) > Cu(II) > Zn(II) > Mn(II) > Cd(II) which almost matches the obtained data, so that the sorption capacity strength is impacted positively with the increase of the metal ion hydration energy. This means that the sorption affinity could be correlated to this parameter. The same observation has been reported by Igwe and Abia (2007). The electronegativity of manganese, copper, zinc, cadmium, and uranium metal ions is 1.55, 1.90, 1.65, 1.69, and 1.38, respectively, so that the resin affinity towards the metal ions should be arranged as Cu(II) > Cd(II) > Zn(II) > Mn(II) > U(VI) which is inconsistent with the obtained results. This indicated that the resin affinity could not be correlated to this parameter where it has not critical influence on the metal ion sorption tendency. The hydrolysis constant (PK_a) of the metal ions could be sequenced as the following: Mn(II) 10.7 > Cd(II) 10.01 > Zn(II) 9.15 > Cu(II) 7.62 > U(VI) 5.19. It is obvious that the resin affinity is almost affected positively with the decrease of the metal ion hydrolysis constant. This behavior disagrees with Mihajlović et al. (2014).

The differences in the metal-binding strength can be interpreted using the classification of metal ions according to the Pearson Hard and Soft Acids and Bases (HSAB) theory, which considered the metal ions behave as acids (i.e., electron acceptors) and the functional group ligands in resins as bases (i.e., electron donors) following the Lewis theory of acids and bases (Pearson 1966; Demey et al. 2018). Strong acid will preferentially react with strong bases and reciprocal: weak acids with weak bases. Based on HSAB theory, uranium is classified as hard acid; however, cadmium is considered as soft acid, and zinc, copper, and manganese are considered as borderline (Demey et al. 2018). The Lewis acid strength of uranium, zinc, copper, manganese, and cadmium are 0.868, 0.405, 0.374, 0.334, and 0.32, respectively (Gagné and Hawthorne 2017). This means that the affinity of the sulfonic group of the Marathon C resin will be ordered as the following: uranium > zinc > copper > manganese > cadmium ions. This ranking is the same sequence obtained from the experimental results, which indicates that the results obtained from experimental work are in agreement with the HSBA theory.

The sorption performance of Marathon C resin for U(VI), Mn(II), Cu(II), Zn(II), and Cd(II) has been compared with other sorbents and displayed in Table 4. From the table, it is clear that the kinetic performance of Marathon C resin is moderate in regards to the presented sorbents. In addition, Marathon C resin displays the highest sorption capacity for U(VI), Mn(II), and Cu(II) ions comparable with the alternative materials; however, Fe-pillared Tunisian bentonite shows higher sorption capacity for Zn(II) and Amberlite XAD-7-Cyanex-301explor higher sorption capacity for Cd(II) ions. Nevertheless, Marathon C exhibits the following advantages: as a commercial resin, it is characterized by heat and acid resistances and the ability to reuse for several sorption-desorption cycles (Nagaphani Kumar et al. 2010; Hérès et al. 2018).

Effect of contact time

The rate of reaction is considered as one of the main parameters that can control the scaling-up of the sorption process. In this concern, the impact of contact time on U(VI), Mn(II), Cd(II), Zn(II), and Cu(II) sorption from multi-component phosphoric acid solution has been investigated using Marathon C resin. The experimental conditions of the sorption process were kept at 4.0 g/L and sorbent dose; 2.0 M phosphoric acid solution contains 50 mg/L of each metal ions and room temperature while the contact time was ranged from 2.0 to 600.0 min. Figure 5 represents the metal ion sorption efficiency as a function of reaction time. The obtained data display that the sorption started with a fast rate of interreaction until the equilibrium was noted, and then a slow rate had taken place. The five metal ions exhibit the same behavior. The first period of reaction, fast rate, could be owing to the availability of active groups on Marathon C resin. Nevertheless, at equilibrium, most of the resin active sites on the surface are almost occupied by U(VI), Mn(II), Cd(II), Zn(II), and Cu(II) ions; thus, the ions react with the inside active groups, which take more time (Zhang et al. 2015; Taha et al. 2019).

Figure 5 also clear that the sorption percent of Cu(II), Zn(II), and U(VI) ions improved with the increase of contact

Table 4 Comparison of sorption performance of U(VI), Mn(II), Cu(II), Zn(II), and Cd(II) for different sorbents

Sorbent	$[H_3PO_4]$, M	Time, h	q_m, mg/g					Ref
			U(VI)	Mn(II)	Cu(II)	Zn(II)	Cd(II)	
MARATHON C resin	2.0	2.0–4.0	14.77	9.48	11.1	13.05	7.29	This work
0.05 M Triphenylphosphine sulfide impregnated charcoal	3.5	2.0	n.r.	n.r.	1.74	1.83	2.88	El-Sofany et al. (2009)
0.1 M Triphenylphosphine sulfide impregnated charcoal	3.5	2.0	n.r.	n.r.	3.7	9.43	4.18	El-Sofany et al. (2009)
Tunisian bentonite	1.0	2.0	n.r.	n.r.	0.47	n.r.	n.r.	Abdennebi et al. (2013)
White silica sand	5.0	24.0	0.14	n.r.	n.r.	n.r.	n.r.	El-Bayaa et al. (2011)
Abu Zenima white sand	5.1	24.0	0.87	n.r.	n.r.	2.22	0.14	Cheira et al. (2014)
Raw bentonite clay	8.8	2.0	n.r.	n.r.	n.r.	7.08	n.r.	Hamza et al. (2016)
Fe-pillared Tunisian bentonite	8.8	1.5	n.r	n.r	n.r	14.09	n.r.	Hamza et al. (2016)
Posidonia oceanica impregnated kaolinite	8.5	96.0	n.r.	n.r.	n.r.	n.r.	2.02	Omri and Batis (2013)
K10 montmorillonite modified by EDTA	8.5	96.0	n.r	n.r	n.r	n.r	2.68	Omri and Batis (2013)
K10 montmorillonite modified by iron oxide	8.5	96.0	n.r.	n.r.	n.r.	n.r.	1.73	Omri and Batis (2013)
Amberlite XAD-2-Cyanex-301	3.2	0.8	n.r	n.r	n.r	n.r	1.56	Hinojosa Reyes et al. (2001)
Amberlite XAD-7-Cyanex-301	12.7	4.0	n.r	n.r	n.r	n.r	11.52	Hinojosa Reyes et al. (2001)
Metakaolinite	5.5	1.0	1.02	n.r	n.r	n.r	n.r	Taha et al. (2018)
Kaolinite	5.5	1.0	0.65	n.r.	n.r.	n.r.	n.r.	Taha et al. (2018)
D2EHPA-impregnated charcoal	4.5	1.0	0.47	n.r.	n.r.	n.r.	n.r.	Ali et al. (2013)

n.r. not reported

time and reached a steady state at 120 min. Numerically, the sorption efficiency was about 77.8, 80.6, 83.1% for Zn(II), U(VI), and Cu(II)ions, respectively. There is no remarkable increase in the sorption efficiency observed after the equilibrium time. However, the equilibrium time of Mn(II) and Cd(II) ions was obtained at 240 min where the sorption efficiency was about 77.1 and 65.1%, respectively. The further increase of the reaction time could yield a slight impact on the sorption efficiency.

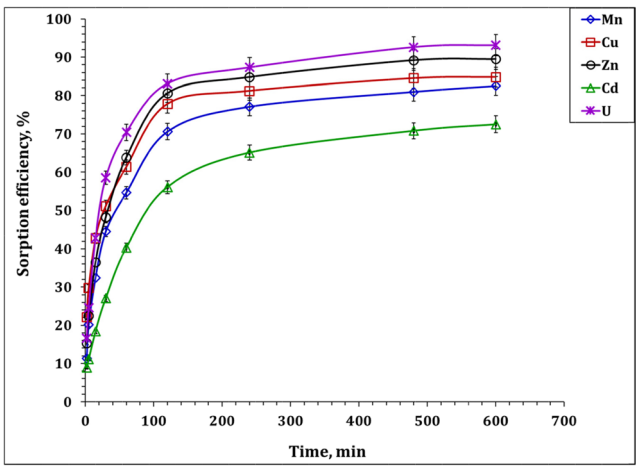

Fig. 5 Impact of shaken time on U(VI), Mn (II), Cd(II), Zn(II), and Cu(II) sorption efficiency, % (4.0 g sorbent/L of 2.0 M phosphoric acid; temperature 298 K; 100 rpm)

The kinetics of U(VI), Mn(II), Cd(II), Zn(II), and Cu(II) ions using Marathon C resin have been figured out by analyzing the obtained data using the non-linear equations of Lagergren, pseudo-second-order, Elvoich kinetic models. The kinetic curves for the adsorption process are displayed in Fig. 6. The parameters of the investigated kinetic models as well as the Chi-square coefficient and the average relative error have been evaluated and displayed in Table 5. The kinetic analysis for the obtained data (Fig. 6) confirm the increase of the sorption capacity of U(VI), Zn(II), and Cu(II) ions up to about 120 min (equilibrium state) and 240 min for Mn(II) and Cd(II).

The obtained data in Table 5 declare that the pseudo-second-order model exhibits the lowest Chi-square coefficient and the lowest average relative error for the investigated five metal ions. This declared that the sorption of Mn(II), Cu(II), Zn(II), Cd(II), and U(VI) ions from the phosphoric acid solution using Marathon C resin obeyed to McKay equation which indicates that the rate-controlling step is chemisorption. The sorption process has occurred through a chemical reaction, an electronic sharing, or an electronic gain between the resin and the metal ions (Wekoye et al. 2020; Tan and Hameed 2017). The rate constant of Cu(II) is the highest among the five investigated metal ions (0.0059 min^{-1}), followed by U(VI)

Table 5 The values of Lagergren, McKay, and Elovich kinetic equation parameters

	Mn	Cu	Zn	Cd	U
Pseudo-first-order model					
q_1 (mg/g)	9.6	10.2	10.6	8.3	10.9
k_1 (min^{-1})	0.03	0.03	0.03	0.02	0.04
X^2	3.0	10.4	4.9	4.2	3.3
ARE (%)	17.9	20.6	17.8	20.0	15.8
Pseudo-second-order model					
q_2 (mg/g)	10.6	10.9	11.7	9.8	12.0
$k_2 \times 10^3$ (min^{-1})	3.80	5.91	3.65	2.07	4.47
h (mol/g/h^{-1})	0.43	0.70	0.50	0.20	0.64
$t_{1/2}$ (h)	24.8	15.6	23.4	49.2	18.6
X^2	0.9	2.5	1.4	1.7	0.8
ARE (%)	10.0	12.3	10.8	13.2	7.7
Elovich model					
b (mg/g/min)	1.07	3.55	1.45	0.41	2.00
a (g/mg)	0.63	0.83	0.63	0.67	0.60
X^2	1.3	2.9	2.2	2.3	1.7
ARE (%)	11.3	17.0	13.2	17.4	11.4

which has 0.0044 min^{-1}. Zn(II) and Mn(II) ions have the same rate constant (0.0037 min^{-1}); however, the lowest rate of reaction belongs to Cd(II) (0.002 min^{-1}). Cu(II) ions and U(VI) ions have the highest initial adsorption rate (0.70 and 0.64 mol/g/h, respectively), followed by Zn(II) and Mn(II) (0.50 and 0.43 mol/g/h, respectively) while Cd(II) has the lowest initial adsorption rate (0.20 mol/g/h). On the other hand, the half-equilibrium time has the following order: Cd(II) > Mn(II) > Zn(II) > U(VI) > Cu(II) ions. These observations confirm the obtained results that regard that Cu(II), U(VI), and Zn(II) have faster equilibrium and in turn have a higher rate constant than Mn(II) and Cd(II). Marathon C resin has a different affinity at equilibrium towards the investigated metal ions as indicated in Table 5. The resin affinity towards the metal ions could be ranked as the following: U(VI) > Zn(II) > Cu(II) > Mn(II) > Cd(II) ions. Numerically, the sorption capacity for the studied metal ions was equal 12.0, 11.7, 10.9, 10.6, and 9.8 mg/g for U(VI), Zn(II), Cu(II), Mn(II), Cd(II) ions, respectively.

The reaction kinetic models, namely, Lagergren, McKay, and Elovich, could not explain the diffusion mechanism of U(VI), Mn(II), Cd(II), Zn(II), and Cu(II) ion sorption reaction; accordingly, the diffusion mechanism has been explored by applying the intraparticle diffusion kinetic equation (IPD) (Wekoye et al. 2020). The analysis of the obtained results using Morris-Weber model declared that the IPD illustrate consists of two stages (multi-linear relationship) for the five metal ions (Fig. 7). This means that the intraparticle diffusion of U(VI), Mn(II), Cd(II), Zn(II), and Cu(II) species through the resin bead was not the only mechanism of the sorption process (Wu et al. 2009). This could be attributed to that the rate of mass transfer in the initial and the final stages of the sorption are not the same which makes the effect of the boundary layer obvious (Wekoye et al. 2020). Generally, every linear segment represents a controlling mechanism or numerous simultaneous controlling mechanisms (Wekoye et al. 2020). The first stage has a high adsorption rate ki and low boundary layer effect, which confirmed the fast reaction at this stage. This could be attributed to the availability of sorption sites on the solid surface; therefore, the external surface adsorption occurs (Wu et al. 2009).

The parameters of the IPD model were evaluated and explored in Table 6. From the table, it is clear that U(VI) and Zn(II) have the highest reaction rate constant (0.88 and 0.86 mg/g $min^{1/2}$, respectively) followed by Mn(II) and Cu(II) (0.76 and 0.71 mg/g/$min^{1/2}$, respectively); however, Cd(II) has the lowest sorption rate of reaction (0.64 mg/g/$min^{1/2}$). Nevertheless, the second stage is characterized by

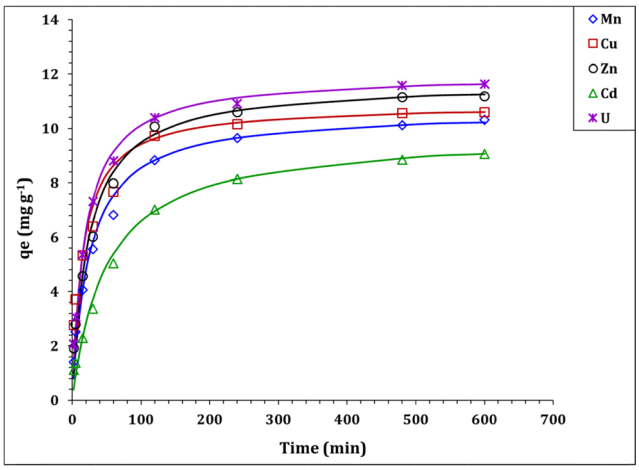

Fig. 6 Pseudo-second-order plot for U(VI), Mn(II), Cd(II), Zn(II), and Cu(II) sorption from phosphoric acid solution using Marathon C resin

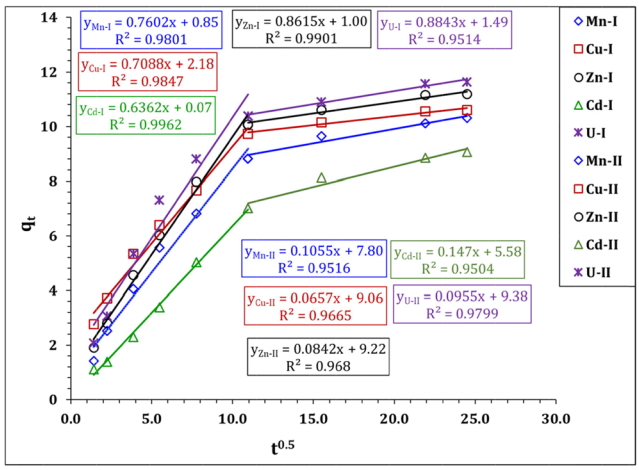

Fig. 7 Morris-Weber illustration for U(VI), Mn(II), Cd(II), Zn(II), and Cu(II) adsorption from phosphoric acid solution using Marathon C resin

Table 6 The values of Morris-Weber model parameters

		Mn	Cu	Zn	Cd	U
Weber and Morris model	Stage I					
	k_i (mg/g/min$^{1/2}$)	0.76	0.71	0.86	0.64	0.88
	C	0.9	2.2	1.0	0.1	1.5
	R^2	0.98	0.98	0.99	0.99	0.95
	Stage II					
	k_i (mg/g/min$^{1/2}$)	0.11	0.07	0.08	0.15	0.10
	C	7.8	9.1	9.2	5.6	9.4
	R^2	0.95	0.96	0.96	0.95	0.97

the low adsorption reaction rate and high boundary layer effect, which confirm the slowdown of the speed of reaction at this stage. This behavior is due to the saturation of most of the surface sorbent sites; therefore, the adsorption occurs by the intra-particle sorbent sites (Wu et al. 2009). At the second stage, Cd(II) has the highest ki followed by Mn(II) and U(VI) (0.15, 0.11, and 0.10 mg/g/min$^{1/2}$, respectively) and Cu(II) and Zn(II) have the lowest ki (0.07 and 0.08 mg/g/min$^{1/2}$, respectively).

Effect of phosphoric acid concentration

The performance of U(VI), Mn(II), Cd(II), Zn(II), and Cu(II) ion removal from phosphoric acid solution as a function of phosphoric acid molarity ranging from 1.0 to 6.0 M is studied and illustrated in Fig. 8. The experimental conditions were Marathon C resin dose of 4.0 g/L, initial metal ion concentration of 50 mg/L, room temperature, and contact time of 10 h. The revealed results in Fig. 8 indicated that the sorption efficiency of U(VI), Zn(II), and Cu(II) has gradually decreased with the increase of phosphoric acid molarity. However, the sorption efficiency of Mn(II) and Cd(II) has dramatically

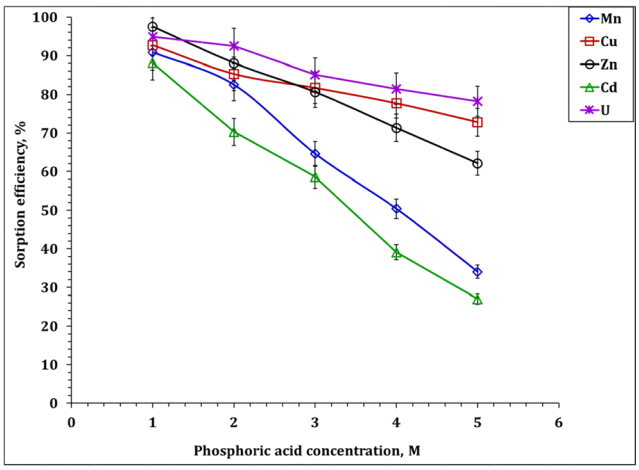

Fig. 8 Impact of phosphoric acid molarity on U(VI), Mn(II), Cd(II), Zn(II), and Cu(II) sorption efficiency, % (4.0 g sorbent/L of phosphoric acid; temperature 298 K; 100 rpm)

decreased with the raise of phosphoric acid concentration. Numerically, U(VI) has the lowest effect with the increase of acid concentration where its sorption efficiency decreased from about 95 to 73%, followed by Cu(II), which decreased from about 93 to 63%. Zn(II) metal ion is in the middle, where its sorption percent decreased by about 50% (97% to 50%) within the increase of phosphoric acid concentration. However, the increase in phosphoric acid concentration drastically reduces the sorption efficiency of Mn (II) and Cd(II) ions, where their sorption percent decreased from about 91 to 24% for Mn(II) and from about 88 to 18% for Cd(II).

The sorption efficiency decreases with the increase of the phosphoric acid concentration indicating that the sorption follows ion exchange type mechanism (Nagaphani Kumar et al. 2010); however, at high hydrogen ion concentrations, the decrease in the sorption efficiency suggests a change in the sorption mechanism (Canner et al. 2018). This suggestion is consistent with the mathematical treatment of the obtained results using Morris-Weber model kinetic model (Fig. 4), which indicated the presence of several mechanisms that control the sorption process. The difference in the degree of phosphoric acid impact on the sorption percent for the five metal ions could be due to different speciation of the metal ions in the phosphoric acid. Accordingly, MEDUSA software was used to figure out the species of the investigated metal ions (50 mg/L) in phosphoric acid concentration 2.0 M (Fig. 9).

The speciation of the metal ions using MEDUSA software (Fig. 9) shows that the investigated metal ions explore different species. Specifically, uranium exhibited different cationic, anionic, and neutral species $[(UO_2(H_2PO_4)(H_3PO_4)]^+$, $[UO_2(H_2PO_4)]^+$, $[UO_2(H_3PO_4)]^{2+}$, $UO_2(H_2PO_4)_2$, $UO_2(HPO_4)\cdot 4H_2O$, $UO_2(OH)_2\cdot H_2O$, $[UO_2(PO_4)]^-$, $[UO_2(OH)_3]^-$, $[UO_2(OH)_4]^{2-}$, $[UO_2(H_2PO_4)(H_3PO_4)]^+$). Copper also displayed numerous cationic, anionic, and neutral species (Cu^{2+}, $[Cu(H_2PO_4)]^+$,$Cu(H_2PO_4)_2$, $Cu(HPO_4)$, $[Cu(H_2PO_4)_2(HPO_4)]^{2-}$, $[Cu(HPO_4)_2]^{2-}$, CuO). Cadmium also showed several cationic and neutral species (Cd^{2+}, $[Cd(H_2PO_4)]^+$, $Cd(HPO_4)$, $Cd_5(HPO_4)_2(PO_4)_2\cdot 4H_2O$, $Cd_3(PO_4)_2$). Zinc and manganese explored only cationic and neutral species as the following (Zn^{2+}, $Zn_3(PO_4)_2\cdot 4H_2O$,

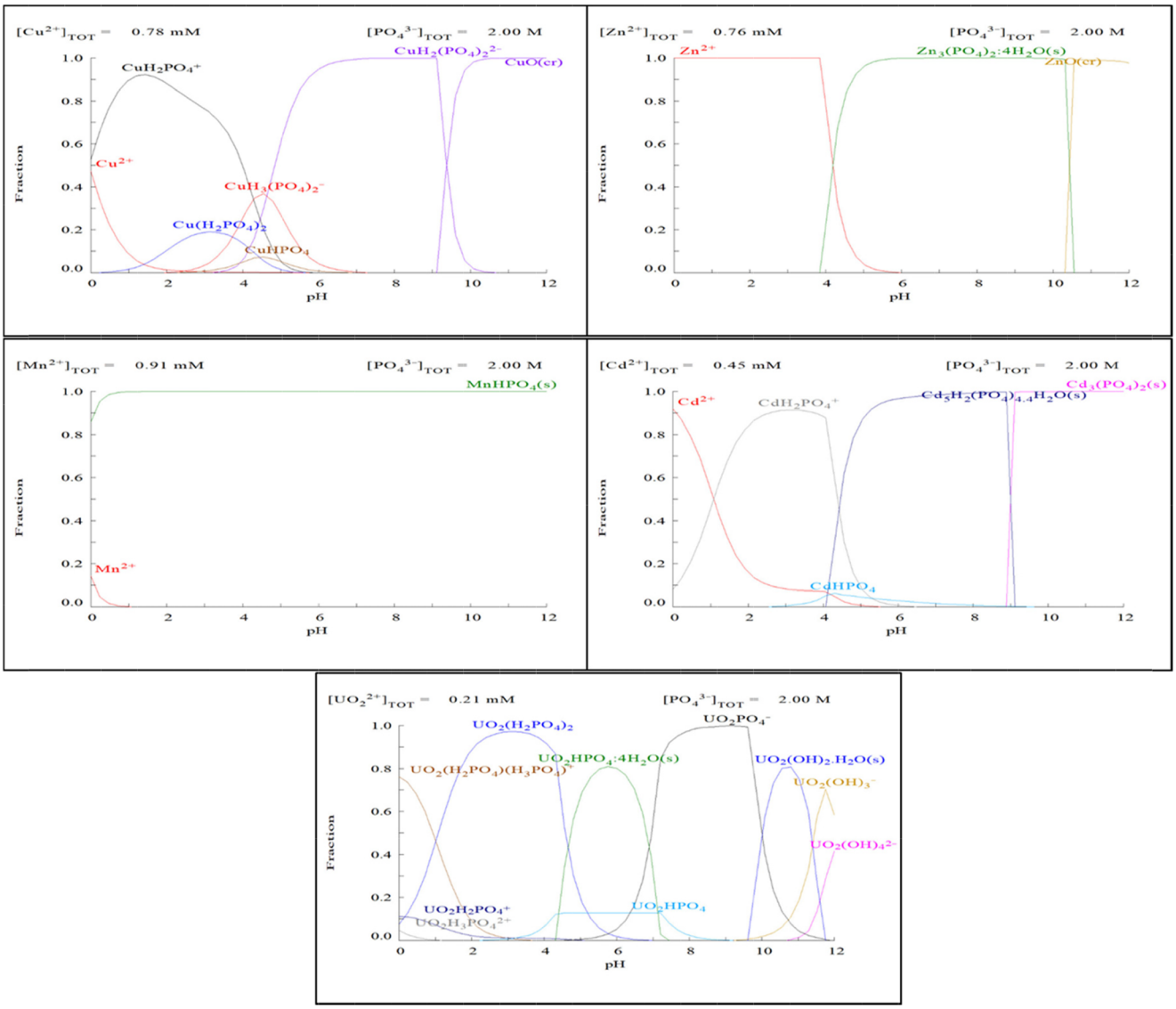

Fig. 9 Metal ion species calculated by Hydra/Medusa (phosphoric acid molarity is 2.0 M and metal ion concentration is 50 mg/L)

ZnO) and (Mn^{2+}, $MnHPO_4$). The main predominate species of the metal ions within the phosphoric acid molarity ranging from 1.0 to 6.0 M (pH ranging from 1.0 to 0.6, respectively) were $[CuH_2PO_4]^+$, $[UO_2(H_2PO_4)H_3PO_4]^+$, Zn^{2+}, Mn^{2+}, Cd^{2+}. This displays that both uranium and copper form stable complexes with phosphoric acid at phosphoric acid concentration of 2.0 M while other metal ions form free ionic species. In addition, it could be proposed that the monovalent cationic species will be exchanged with only one H^+ from the resin while other divalent free cationic species will require two H^+ ions from the resin. The relation between Log K_d (distribution coefficient) and Log acid molarity (Fig. 10) displayed linear relationship for the five metal ions with different slopes.

The slope of this relationship is generally present in the ion exchange processes with the stoichiometry of proton ion exchange. Cu(II) and U(VI) exhibit slopes close to 1, while Mn(II), Zn(II), and Cd(II) show slopes close to 2. These

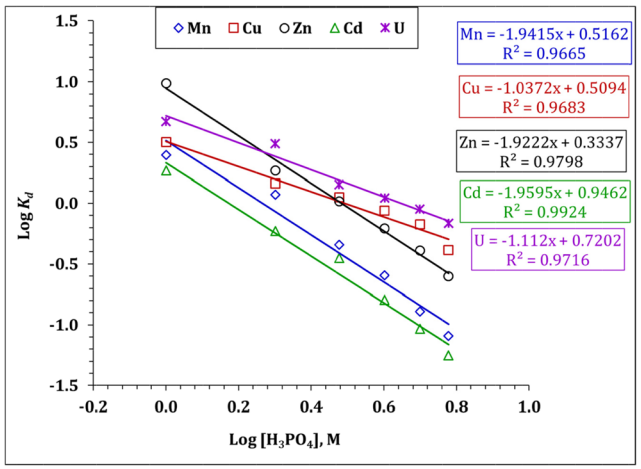

Fig. 10 The relation between Log K_d and Log phosphoric acid molarity

results are consistent with the obtained metal ion species in Fig. 9. In this regard, the binding of the resin with the metal ions could be proposed as in Fig. 11.

Application to polishing of commercial phosphoric acid

Crude phosphoric acid contains a high level of toxic and radioactive elements which are in turn inappropriate for the manufacturing of fertilizers. In this respect, Marathon C resin has been applied batch-wise for polishing crude industrial phosphoric acid supplied by AZFC in order to produce an appropriate phosphoric acid for the production of eco-friendly fertilizers. The polishing experiment has been performed based on the following conditions: phosphoric acid concentration of 23.5% P_2O_5, sorbent amount of addition is 4.0 g/L, contact time of 24 h, and room temperature. Subsequent filtration was achieved. The chemical specifications of the treated commercial phosphoric acid are given in Table 7.

The acquired results are obvious that Marathon C resin has no effect on the concentration of P_2O_5, sulfate, and fluoride. Nevertheless, the concentrations of Fe_2O_3, SiO_2, and MgO have been reduced from 1.2 to 1.0 for Fe_2O_3, from 0.08 to 0.07 for SiO_2, and from 0.8 to 0.6 for MgO. This could be attributed to that Fe^{3+}, Si^{4+}, and Mg^{2+} ions are considered as hard metal according to HSAB. Manganese concentration has been changed from 580 to 484 mg/L (about 16.5% removal efficiency). The removal efficiency of zinc was about 25%. For uranium, copper, and cadmium ions, the sorption efficiency was about 90.2, 82.2, and 80.6%, respectively. In the comparison between Marathon C resin sorption efficiency for manganese, copper, zinc, cadmium, and uranium ions from synthetic phosphoric acid solution (case 1) and industrial phosphoric acid (case 2), it is noticeable that the sorption efficiency of manganese and zinc in case 2 is dramatically decreased than case 1. This could be attributed to that crude phosphoric acid contains an extremely high concentration of metal ions as well as organic compounds, which results in high saturation of the resin and in turn decreases the sorption efficiency. Nevertheless, the resin exhibits high sorption efficiency for uranium, copper, and cadmium ions in both cases, which could be explained by much lower concentration in phosphoric acid. There is no doubt that the commercial resin, Marathon C, has a limited effect on the huge concentration of impurities in industrial phosphoric acid. However, crude phosphoric acid after treatment with Marathon C resin becomes appropriate for the production of eco-friendly phosphate fertilizers: manganese, copper, zinc, cadmium, and uranium ion concentrations are about 1590, 31, 450, 10, and 13 mg/kg P_2O_5 that is acceptable with respect to the levels recommended by The German Fertilizer Ordinance for 2008 (Kratz et al. 2016; Kratz et al. 2012).

Table 7 Specifications of crude phosphoric acid before and after contact with resins

Compound	Initial content	After contact with the resin
Concentration Wt.%		
P_2O_5	≈ 23.5	≈ 23.5
Fe_2O_3	1.2	1.0
CaO	0.34	0.3
SO_4	1.35	1.35
MgO	0.8	0.6
SiO_2	0.08	0.07
F	0.5	0.5
Concentration (mg/L)		
Cd	10.5	3.1
Mn	580	484.9
Cu	53	9.5
Zn	183	137.4
U	41	4.0

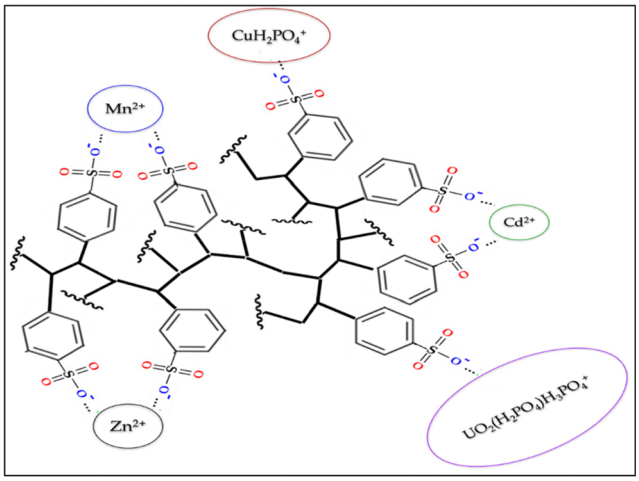

Fig. 11 The proposed binding between the resin and U(VI), Mn(II), Cd(II), Zn(II), and Cu(II) ions

Conclusion

In this study, a strong cation exchange resin, Marathon C, has been tested for the sorption of U(VI), Mn(II), Cd(II), Zn(II), and Cu(II) ions from multi-component phosphoric acid solutions. The explored results revealed that the sorption of the five metals is strongly affected by the variation of resin amount of addition, reaction time, ion initial concentration, and phosphoric acid molarity. The uptake kinetics for all investigated metal ions has been fitted well by the non-linear equation of pseudo-second-order kinetic model, which means that the sorption process was chemisorption. The isotherm analysis for the obtained data shows that the sorption process

obeys Langmuir model. The sorption capacity of Marathon C resin could be arranged as the following: U(VI) > Zn(II) > Cu(II) > Mn(II) > Cd(II) ions. The result has highlighted opportunities for the application of cation exchange resins in the hydrometallurgical processing of phosphoric acid clarification and in turn the production of eco-friendly phosphate fertilizers.

Authors' contributions Not applicable.

Data availability The datasets used and/or analyzed during the current study are available from the corresponding author on reasonable request.

Compliance with ethical standards

Competing interest The authors declare that they have no competing interest.

Ethical approval Not applicable.

Consent to participate Not applicable.

Consent to publish Not applicable.

References

Abdennebi N, Bagane M, Chtara C (2013) Removal of copper from phosphoric acid by adsorption on Tunisian bentonite 4(6). doi: https://doi.org/10.4172/2157-7048.1000166,04

Al-Ghouti MA, Da'ana DA (2020) Guidelines for the use and interpretation of adsorption isotherm models: a review. J Hazard Mater 393: 122383. https://doi.org/10.1016/j.jhazmat.2020.122383

Al-Harahsheh M, Hussain YA, Al-Zoubi H, Batiha M, Hammouri E (2017) Hybrid precipitation-nanofiltration treatment of effluent pond water from phosphoric acid industry. Desalination 406:88–97. https://doi.org/10.1016/j.desal.2016.06.014

Ali MM, Taha MH, Kandil KM, Al-Zughbi AA, Musa MA (2013) Kinetics and thermodynamics of uranium adsorption from commercial di-hydrate phosphoric acid using D2EHPA-impregnated charcoal 46(5):29–37

Ayawei N, Ebelegi AN, Wankasi D (2017) Modelling and interpretation of adsorption isotherms. J Chem 2017:1–11. https://doi.org/10.1155/2017/3039817

Bahrpaima K (2017) Purification of phosphoric acid by liquid-liquid equilibrium. In: Wiener MS, Valdez B (eds) Phosphoric acid industry - problems and solutions. InTech

Canner AJ, Pepper SE, Hayer M, Ogden MD (2018) Removal of radionuclides from a HCl steel decontamination stream using chelating ion exchange resins – initial studies. Prog Nucl Energy 104:271–279. https://doi.org/10.1016/j.pnucene.2017.10.007

Cheira MF (2015) Characteristics of uranium recovery from phosphoric acid by an aminophosphonic resin and application to wet process phosphoric acid. Eur J Chem 6(1):48–56. https://doi.org/10.5155/eurjchem.6.1.48-56.1143

Cheira MF, Ibrahium HZ, Elsayd AM (2014) Potentiality of white sand for the purification of wet process phosphoric acid from some metallic elements (U, Zn, Cd) 9(6):224–233

Chen A, Zhu J, Wu B, Chen K, Ji L (2012) Continuous melt suspension crystallization of phosphoric acid. JCPT 02(03):111–116. https://doi.org/10.4236/jcpt.2012.23014

Demey H, Vincent T, Guibal E (2018) A novel algal-based sorbent for heavy metal removal. Chem Eng J 332:582–595. https://doi.org/10.1016/j.cej.2017.09.083

El-Bayaa AA, Badawy NA, Gamal AM, Zidan IH, Mowafy AR (2011) Purification of wet process phosphoric acid by decreasing iron and uranium using white silica sand. J Hazard Mater 190(1–3):324–329. https://doi.org/10.1016/j.jhazmat.2011.03.037

Elleuch MBC, Amor MB, Pourcelly G (2006) Phosphoric acid purification by a membrane process: electrodeionization on ion-exchange textiles. Sep Purif Technol 51(3):285–290. https://doi.org/10.1016/j.seppur.2006.02.009

El-Sofany EA, Zaher WF, Aly HF (2009) Sorption potential of impregnated charcoal for removal of heavy metals from phosphoric acid. J Hazard Mater 165(1–3):623–629. https://doi.org/10.1016/j.jhazmat.2008.10.037

Fayiga AO, Nwoke OC (2016) Phosphate rock: origin, importance, environmental impacts, and future roles. Environ Rev 24(4):403–415. https://doi.org/10.1139/er-2016-0003

Foo KY, Hameed BH (2010) Insights into the modeling of adsorption isotherm systems. Chem Eng J 156(1):2–10. https://doi.org/10.1016/j.cej.2009.09.013

Gaafar I, El-Shershaby A, Zeidan I, El-Ahll LS (2016) Natural radioactivity and radiation hazard assessment of phosphate mining, Quseir-Safaga area, Central Eastern Desert, Egypt. NRIAG J Astron Geophys 5(1):160–172. https://doi.org/10.1016/j.nrjag.2016.02.002

Gagné OC, Hawthorne FC (2017) Empirical Lewis acid strengths for 135 cations bonded to oxygen. Acta Crystallogr Sect B: Struct Sci Cryst Eng Mater 73(Pt 5):956–961. https://doi.org/10.1107/S2052520617010988

Geissler B, Mew MC, Weber O, Steiner G (2015) Efficiency performance of the world's leading corporations in phosphate rock mining. Resour Conserv Recycl 105:246–258. https://doi.org/10.1016/j.resconrec.2015.10.008

Geissler B, Mew MC, Steiner G (2019) Phosphate supply security for importing countries: developments and the current situation. Sci Total Environ 677:511–523. https://doi.org/10.1016/j.scitotenv.2019.04.356

Hagag MA, El-Gayar DA, Nosier SA, Mubark AA (2017) Removal of heavy metals from industrial waste solutions by a rotating fixed bed of ion exchange resin. Desalin Water Treat 100:178–184. https://doi.org/10.5004/dwt.2017.21794

Hamza W, Chtara C, Benzina M (2016) Purification of industrial phosphoric acid (54%) using Fe-pillared bentonite. Environ Sci Pollut Res 23(16):15820–15831. https://doi.org/10.1007/s11356-015-5557-5

Hérès X, Blet V, Di Natale P, Ouaattou A, Mazouz H, Dhiba D, Cuer F (2018) Selective extraction of rare earth elements from phosphoric acid by ion exchange resins. Metals 8(9):682. https://doi.org/10.3390/met8090682

Hinojosa Reyes L, Saucedo Medina I, Navarro Mendoza R, Revilla Vázquez J, Avila Rodríguez M, Guibal E (2001) Extraction of cadmium from phosphoric acid using resins impregnated with organophosphorus extractants. Ind Eng Chem Res 40(5):1422–1433. https://doi.org/10.1021/ie0005349

Hocking MB (2005) Phosphorus and phosphoric acid. In: Handbook of Chemical Technology and Pollution Control. Elsevier, pp. 289–320

Hussein AEM, Taha MH (2013) Uranium removal from nitric acid raffinate solution by solvent immobilized PVC cement. J Radioanal Nucl Chem 295(1):709–715. https://doi.org/10.1007/s10967-012-2158-3

Igwe JC, Abia AA (2007) Adsorption isotherm studies of Cd (II), Pb (II) and Zn (II) ions bioremediation from aqueous solution using unmodified and EDTA-modified maize cob. Eclética Química 32: 33–42

Jaafari J, Yaghmaeian K (2019a) Optimization of heavy metal biosorption onto freshwater algae (Chlorella coloniales) using

response surface methodology (RSM). Chemosphere 217:447–455. https://doi.org/10.1016/j.chemosphere.2018.10.205

Jaafari J, Yaghmaeian K (2019b) Response surface methodological approach for optimizing heavy metal biosorption by the blue-green alga. Chroococcus Disperses 142:225–234. https://doi.org/10.5004/dwt.2019.23406

Khalili FI, Salameh N'aH, Shaybe MM (2013) Sorption of uranium(VI) and thorium(IV) by Jordanian Bentonite. J Chem 2013:1–13. https://doi.org/10.1155/2013/586136

KOOPMAN C, WITKAMP GJ, van ROSMALEN GM (1999) Removal of heavy metals and lanthanides from industrial phosphoric acid process liquors. Sep Sci Technol 34(15):2997–3008. https://doi.org/10.1081/SS-100100818

Kratz S, Godlinski F, Schnug E (2012) Heavy metal loads to agricultural soils in Germany from the application of commercial phosphorus fertilizers and their contribution to background concentration in soils. In: Merkel B, Schipek M (eds) The new uranium mining boom: challenge and lessons learned. Springer, Berlin Heidelberg, Berlin, Heidelberg, pp 755–762

Kratz S, Schick J, Schnug E (2016) Trace elements in rock phosphates and P containing mineral and organo-mineral fertilizers sold in Germany. Sci Total Environ 542(Pt B):1013–1019. https://doi.org/10.1016/j.scitotenv.2015.08.046

Largitte L, Pasquier R (2016) A review of the kinetics adsorption models and their application to the adsorption of lead by an activated carbon. Chem Eng Res Des 109:495–504. https://doi.org/10.1016/j.cherd.2016.02.006

Lazarević S, Janković-Častvan I, Jovanović D, Milonjić S, Janaćković D, Petrović R (2007) Adsorption of Pb2+, Cd2+ and Sr2+ ions onto natural and acid-activated sepiolites. Appl Clay Sci 37(1–2):47–57. https://doi.org/10.1016/j.clay.2006.11.008

Machorro JJ, Olvera JC, Larios A, Hernández-Hernández HM, Alcantara-Garduño ME, Orozco G (2013) Electrodialysis of phosphates in industrial-grade phosphoric acid. ISRN Electrochem 2013:1–12. https://doi.org/10.1155/2013/865727

Mar SS, Okazaki M (2012) Investigation of Cd contents in several phosphate rocks used for the production of fertilizer. Microchem J 104:17–21. https://doi.org/10.1016/j.microc.2012.03.020

Marczenko Z, Balcerzak M (2000) Uranium. In: Separation, Preconcentration and Spectrophotometry in Inorganic Analysis, vol 10. Elsevier, pp 446–455

Marques BS, Frantz TS, Junior S'AC, Roberto T, de Almeida Pinto LA, Dotto GL (2019) Adsorption of a textile dye onto piaçava fibers: kinetic, equilibrium, thermodynamics, and application in simulated effluents. Environ Sci Pollut Res 26(28):28584–28592. https://doi.org/10.1007/s11356-018-3587-5

Mihajlović Marija T., Lazarević Slavica S., Janković-Častvan Ivona M., Jokić Bojan M., Janaćković Đorđe T., Petrović Rada D. (2014) A comparative study of the removal of lead, cadmium and zinc ions from aqueous solutions by natural and Fe(III)-modified zeolite. doi: https://doi.org/10.2298/CICEQ121017010M

Moreno JC, Gómez R, Giraldo L (2010) Removal of Mn, Fe, Ni and Cu ions from wastewater using cow bone charcoal. Materials 3(1):452–466. https://doi.org/10.3390/ma3010452

Mousa M. A., Gado H. S., Abd-El Fattah M. M. G., A. E. Madi, Taha M. H., O. E. Roshdy (2013) Removal of uranium from crude phosphoric acid by precipitation technique 46:38–47

Nagaphani Kumar B, Radhika S, Ramachandra Reddy B (2010) Solid–liquid extraction of heavy rare-earths from phosphoric acid solutions using Tulsion CH-96 and T-PAR resins. Chem Eng J 160(1):138–144. https://doi.org/10.1016/j.cej.2010.03.021

Dariush Naghipour, Kamran Taghavi, Mehdi Ashournia, Jalil Jaafari, Ramin Arjmand Movarrekh (2018) A study of Cr(VI) and NH 4+ adsorption using greensand (glauconite) as a low-cost adsorbent from aqueous solutions (1747–6585):1–12. doi: https://doi.org/10.1111/wej.12440

Omri H, Batis NH (2013) Removal of cd(II) from phosphoric acid solution by adsorbents: equilibrium and kinetic studies. Chem Sci Trans 2:357–366

Page MJ, Soldenhoff K, Ogden MD (2017) Comparative study of the application of chelating resins for rare earth recovery. Hydrometallurgy 169:275–281. https://doi.org/10.1016/j.hydromet.2017.02.006

Pearson RG (1966) Acids and bases. Science 151(3707):172–177. https://doi.org/10.1126/science.151.3707.172

Persson I (2010) Hydrated metal ions in aqueous solution: how regular are their structures? Pure Appl Chem 82(10):1901–1917. https://doi.org/10.1351/PAC-CON-09-10-22

Petr Ptáček (ed) (2016) Apatites and their synthetic analogues synthesis, Structure, Properties and Applications

Ridder M de (2012) Risks and opportunities in the global phosphate rock market. Robust strategies in times of uncertainty. Rapport / Centre for Strategic Studies, no. 17 | 12 | 12. The Hague Centre for Strategic Studies, Den Haag

Schoumans OF, Bouraoui F, Kabbe C, Oenema O, van Dijk KC (2015) Phosphorus management in Europe in a changing world. Ambio 44(Suppl 2):S180–S192. https://doi.org/10.1007/s13280-014-0613-9

Smith DW (1977) Ionic hydration enthalpies. J Chem Educ 54(9):540. https://doi.org/10.1021/ed054p540

Steiner G, Geissler B, Watson I, Mew MC (2015) Efficiency developments in phosphate rock mining over the last three decades. Resour Conserv Recycl 105:235–245. https://doi.org/10.1016/j.resconrec.2015.10.004

Mohamed H. Taha (2017) Iron scrubbing from D2EHPA and topo mixture during second cycle of uranium extraction from phosphoric acid using oxalic acid 6:171–180. doi: https://doi.org/10.21608/NSSJ.2017.30780

Taha MH, El-Maadawy MM, Hussein AM, Youssef W (2018) Uranium sorption from commercial phosphoric acid using kaolinite and metakaolinite. J Radioanal Nucl Chem 317:685–699

Taha MH, Abdel Maksoud SA, Ali MM, El Naggar AMA, Morshedy AS, Elzoghby AA (2019) Conversion of biomass residual to acid-modified bio-chars for efficient adsorption of organic pollutants from industrial phosphoric acid: an experimental, kinetic and thermodynamic study. Int J Environ Anal Chem 99(12):1211–1234. https://doi.org/10.1080/03067319.2019.1618459

Tan KL, Hameed BH (2017) Insight into the adsorption kinetics models for the removal of contaminants from aqueous solutions. J Taiwan Inst Chem Eng 74:25–48. https://doi.org/10.1016/j.jtice.2017.01.024

van Kernebeek HRJ, Oosting SJ, van Ittersum MK, Ripoll-Bosch R, de Boer IJM (2018) Closing the phosphorus cycle in a food system: insights from a modelling exercise. Anim :Int J anim Biosci 12(8):1755–1765. https://doi.org/10.1017/S1751731118001039

Vico LI (2003) Acid–base behaviour and Cu2+ and Zn2+ complexation properties of the sepiolite/water interface. Chem Geol 198(3–4):213–222. https://doi.org/10.1016/S0009-2541(03)00002-0

Wang P, Yin L, Wang J, Xu C, Liang Y, Yao W, Wang X, Yu S, Chen J, Sun Y, Wang X (2017) Superior immobilization of U(VI) and 243Am(III) on polyethylenimine modified lamellar carbon nitride composite from water environment. Chem Eng J 326:863–874. https://doi.org/10.1016/j.cej.2017.06.034

Wekoye JN, Wanyonyi WC, Wangila PT, Tonui MK (2020) Kinetic and equilibrium studies of Congo red dye adsorption on cabbage waste

powder. Environ Chem Ecotoxicol 2:24–31. https://doi.org/10.1016/j.enceco.2020.01.004

Wu F-C, Tseng R-L, Juang R-S (2009) Initial behavior of intraparticle diffusion model used in the description of adsorption kinetics. Chem Eng J 153(1–3):1–8. https://doi.org/10.1016/j.cej.2009.04.042

Younes AA, Masoud AM, Taha MH (2018) Uranium sorption from aqueous solutions using polyacrylamide-based chelating sorbents. Sep Sci Technol 53(16):2573–2586. https://doi.org/10.1080/01496395.2018.1467450

Zhang R, Chen C, Li J, Wang X (2015) Preparation of montmorillonite@carbon composite and its application for U(VI) removal from aqueous solution. Appl Surf Sci 349:129–137. https://doi.org/10.1016/j.apsusc.2015.04.222